Korea-Australia Rheology Journal
Vol. 21, No. 4, December 2009 pp. 225-233

The competing roles of extensional viscosity and normal stress differences in complex flows of elastic liquids

K. Walters[1,*], H.R. Tamaddon-Jahromi[2], M.F. Webster[2], M.F. Tomé[3] and S. McKee[4]
[1]*UW Institute of Non-Newtonian Fluid Mechanics, University of Aberystwyth, Aberystwyth, SY23 3BZ, UK*
[2]*UW Institute of Non-Newtonian Fluid Mechanics, Swansea University, School of Engineering, Singleton Park, Swansea, SA28PP, UK*
[3]*Departamento de Matemática Aplicada e Estatística, Universidade de São Paulo, SP, Brazil.*
[4]*Department of Mathematics, University of Strathclyde, Glasgow, Scotland, G1 1XH.*

(Received May 13, 2009; final revision received September 3, 2009)

Abstract

In various attempts to relate the behaviour of highly-elastic liquids in complex flows to their rheometrical behaviour, obvious candidates for study have been the variation of shear viscosity with shear rate, the two normal stress differences N_1 and N_2, especially N_1, and the extensional viscosity η_E. In this paper, we shall be mainly interested in 'constant-viscosity' Boger fluids, and, accordingly, we shall limit attention to N_1 and η_E. We shall concentrate on two important flows - axisymmetric contraction flow and "splashing" (particularly that which arises when a *liquid drop* falls onto the free surface of the same liquid). Modern numerical techniques are employed to provide the theoretical predictions. It is shown that the two obvious manifestations of viscoelastic rheometrical behaviour can sometimes be *opposing* influences in determining flow characteristics. Specifically, in an axisymmetric contraction flow, high η_E can retard the flow, whereas high N_1 can have the opposite effect. In the splashing experiment, high η_E can certainly reduce the height of the so-called Worthington jet, thus confirming some early suggestions, but, again, other rheometrical influences can also have a role to play and the overall picture may not be as clear as it was once envisaged.

Keywords : non-Newtonian fluids, complex flows, contraction flows, splashing, rheometry, constitutive modeling, computational rheology

1. Introduction

1.1. Rheometry

In this communication, we shall be referring frequently to two important 'rheometrical' flows, namely steady simple shear flow and extensional flow. In the former, there is flow only in the x direction and this depends simply and linearly on the y coordinate. *i.e.*

$$v_x = \dot{\gamma} y, \quad v_y = v_z = 0, \tag{1}$$

where v_i is the velocity vector and $\dot{\gamma}$ is the constant shear rate.

For a non-Newtonian elastic liquid, the stress tensor components σ_{ik} can be conveniently written in the form:

$$\begin{aligned} &\sigma_{xy} = \sigma = \dot{\gamma}\eta(\dot{\gamma}), \\ &\sigma_{xx} - \sigma_{yy} = N_1(\dot{\gamma}), \\ &\sigma_{yy} - \sigma_{zz} = N_2(\dot{\gamma}), \end{aligned} \tag{2}$$

where σ is the shear stress, η is the shear viscosity and N_1 and N_2 are the so-called first and second normal stress differences, respectively (Barnes *et al.*, 1989).

For a Newtonian fluid, the stress distribution simply involves one material constant – the coefficient of viscosity η and the two normal stress differences are zero. In the case of a non-Newtonian elastic liquid, η can now be a function of the shear rate, with so-called 'shear thinning' the most commonly observed behaviour. Also, both normal stresses are of potential importance, particularly N_1.

For future reference, we show in Fig. 1 rheometrical data for a so-called Boger fluid (Boger, 1977/1978).

A typical Boger fluid would be a dilute (often a very dilute) solution of a high molecular weight polymer in a very viscous 'Newtonian' solvent. Note that, in the fluid we have taken for illustration purposes, the shear stress (over the shear rates investigated) is taken to be a linear function of $\dot{\gamma}$, *i.e.* the viscosity is constant. Note also that N_1 is much higher than σ, indicating that the fluid is in the 'highly-elastic' category.

For Boger fluids, N_2 is invariably found to be much smaller than N_1 and, in many (most) computational studies, N_2 is taken to be zero.

*Corresponding author: kew@aber.ac.uk

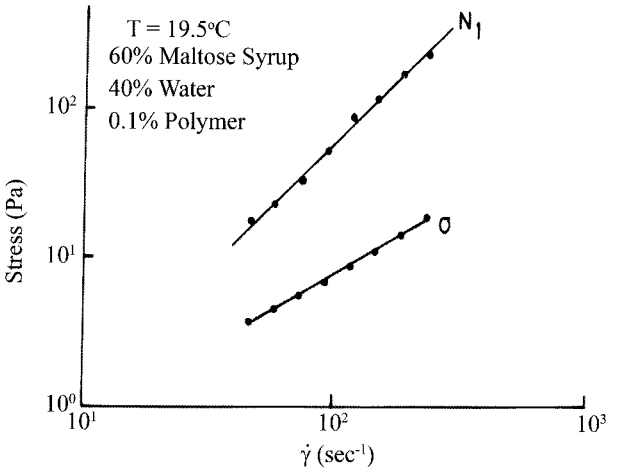

Fig. 1. Rheometrical behaviour of a Boger fluid (see Walters 1980).

At this point it is important to stress that, *from a continuum mechanics standpoint,* the initial dependence of N_1 on $\dot{\gamma}$ has to be quadratic and there is *experimental* evidence (as in Fig. 1) that this quadratic dependence can persist over a reasonable range of shear rates. However, there is also rheometrical evidence available that the dependence of N_1 on $\dot{\gamma}$ can become weaker than quadratic as the shear rate increases further. This is often accompanied by slight shear thinning. For example, in a comprehensive study entitled "A rheometrical study of Boger fluids", Jackson *et al.* (1984) concluded "It will be seen that over a range of shear rates, σ is a linear function of $\dot{\gamma}$ and N_1 is a quadratic function of $\dot{\gamma}$, but that there is a departure from this second-order behaviour at the high shear rates".

The second rheometrical flow of importance in the present study is that called 'uniaxial extensional flow', with a velocity field which can be expressed as

$$v_x = \dot{\varepsilon}x,\ v_y = -\frac{\dot{\varepsilon}y}{2},\ v_z = -\frac{\dot{\varepsilon}z}{2}, \tag{3}$$

where $\dot{\varepsilon}$ is the so-called extensional strain rate. We can write the corresponding stress distribution in the form:

$$\sigma_{xx} - \sigma_{yy} = \sigma_{xx} - \sigma_{zz} = \dot{\varepsilon}\,\eta_E(\dot{\varepsilon}), \tag{4}$$

where η_E is the 'extensional viscosity'. For a Newtonian fluid, $\eta_E = 3\eta$, a result first obtained by Trouton over a hundred years ago (see, for example, Tanner and Walters, 1998). For this reason, the ratio between the two viscosities is called the 'Trouton ratio T_R', and this clearly takes the value 3 for a Newtonian fluid. For a non-Newtonian elastic fluid, T_R can be significantly higher than 3, with 'orders of magnitude' increases not uncommon.

From the above discussion and the relevant literature, we can associate the following rheometrical behaviour with Boger fluids:

1. A reasonably constant shear viscosity η.
2. A potentially high extensional viscosity η_E as the extensional strain rate increases.
3. A high first normal stress difference N_1, which has a quadratic shear rate dependence on $\dot{\gamma}$, at least for small to moderate shear rates.
4. A second normal stress difference N_2 which is negative and at most one tenth of the magnitude of N_1. It is often taken as zero in computational studies.

Clearly, any constitutive model that we use to describe Boger fluids has to satisfy (1)-(4), at least in a semi-quantitative sense.

1.2. Two complex flow

In this communication, we shall concentrate on two (very different) complex flows, which we shall refer to in a generic fashion as 'contraction flows' and 'splashing'.

A schematic of the former is shown in Fig. 2, where both an axisymmetric and a planar contraction are shown (Nigen and Walters, 2002). However, we shall only be considering the former in this work. So, fluid is forced under a pressure gradient through a contraction linking one long cylindrical channel to another of shorter diameter. At specific locations on the walls, upstream and downstream of the contraction, pressure measurements are made. These locations must be far enough from the contraction for the flows to be 'fully-developed' and 'Poiseuille like' at the pressure-measurement stations.

In contraction flows, there is often significant interest in the *kinematics* of the flow structure, particularly the vortices which provide computational rheologists with significant challenges (Walters and Webster, 2003). However, in the present work, we shall confine attention to the *dynamics* of the flow, which is usually studied through the so-called Couette correction C, defined by

$$C = [\Delta p - \Delta p_u L_u - \Delta p_d L_d]/2\sigma_w . \tag{5}$$

This is usually plotted as a function of the Deborah number (or Weissenberg number)

$$\text{De (or We)} = \lambda\dot{\gamma}_w . \tag{6}$$

We shall use the Deborah number and the Weissenberg number interchangeably in various points of this communication. Specifically, we shall use De in the contraction-flow section and We in the splashing section. This reflects

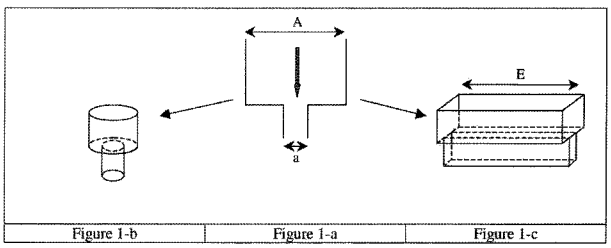

Fig. 2. Schematic diagrams of flow through a planar and an axisymmetric contraction.

the notation used in previous papers on these subjects.

An alternative measure of 'resistance to flow' is the so-called Excess Pressure Drop (*epd*), defined by Binding *et al.* (2006),

$$p^* = \frac{(\Delta p - \Delta p_{fd})_B}{(\Delta p - \Delta p_{fd})_N}, \quad \Delta p_{fd} = \Delta p_u L_u + \Delta p_d L_d \,. \tag{7}$$

In this form, p^* can be equated to the ratio of Couette corrections for constant-viscosity Boger and Newtonian fluids, with corresponding wall shear stress. In the above equations, Δp is the total pressure difference between the inlet and outlet transducers, Δp_u is the fully-developed pressure gradient in the upstream section, Δp_d is the fully-developed pressure gradient in the downstream section, L_u and L_d are their respective lengths, σ_w is the fully-developed wall shear stress in the *downstream* channel. The subscripts N and B represent the corresponding Newtonian and Boger fluid values, respectively, when these are applicable. λ is a characteristic relaxation time and $\dot{\gamma}_w$ is the shear-rate at the downstream wall.

It is well known that, when elastic liquids flow in axisymmetric contractions, large increases in C (or *epd*) can occur. Cogswell (1972), in an influential paper, was clearly guided by such an observation in suggesting that the Couette correction could be used to provide an estimate of extensional viscosity levels, and he provided an analysis to support such a view. This was followed up somewhat later by two important papers by Binding (1988; 1991), the second of which is especially relevant to the ideas we wish to advance in the present paper. This concerns the influence of rheometrical variables such as normal stress differences and extensional viscosity in the determination of the Couette correction. The second Binding paper is especially relevant in this connection and contains the following observation: "The analyses suggest that the effects of elasticity and extensional viscosity are opposite, the former resulting for example in a decreased Couette correction, while the latter causes the Couette correction to increase".

Interestingly, Debbaut and Crochet (1988) and Debbaut *et al.* (1988) reached a very similar conclusion from *computational* work carried out at the same time. Later, we shall have cause to make use of some of the Debbaut and Crochet (1988) ideas. But, at this point, it is sufficient to précis one of their main conclusions: "When the influence of extensional viscosity alone is included, large increases in the Couette correction are predicted. However, these can be hidden and indeed reversed when other rheometrical effects such as large normal stress differences are included".

In our recent computational work on contraction flows (Walters *et al.*, 2008; 2009a, b), we decided to concentrate on the related contraction-expansion (4:1:4) geometry, with rounded corners (see Fig. 3).

We did this for a number of different reasons. For example: (1) We found the geometry to be far easier to handle in the *computations* than the conventional 4:1 geometry with sharp corners. Pressure differences were an order of magnitude lower for the 4:1:4 geometry than with 4:1 geometry flows, with shorter downstream distances demanded to establish relaxed stress beyond the constriction. We have certainly been able to reach higher values of the Deborah number in the simulations. Furthermore, application of the basic numerical method was already well developed in the Swansea research group.

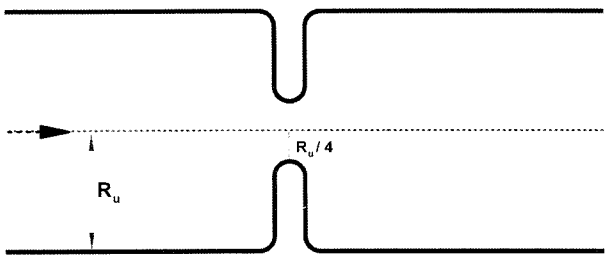

Fig. 3. Schematic diagram of the contraction-expansion geometry with rounded corners.

(2) Importantly, *experimental* data for the 4:1:4 geometry had been supplied by McKinley and his co-workers (Rothstein and McKinley, 2001). These showed the same trends as those already well known in the conventional 4:1 geometry. Of major importance was the appearance in the Rothstein and McKinley experiments of substantial increases in the *epd* for increasing Deborah numbers in the case of Boger fluids.

We now briefly introduce the second type of complex flow we wish to study. In this, either a solid sphere or a liquid drop is released from some distance above the free surface of a liquid. The resulting flow structure is then observed through the use of a high-speed camera.

The resulting splashes can have a rich structure and Fig. 4 shows a schematic representation of some of the features that can occur. The initial crater, the crown structure (with the possibility of distinct satellite drops) and the vertical jet (again with the possibility of distinct satellite drops) are all features that can occur in a single experiment, although it must be stressed that one or more of these features may be

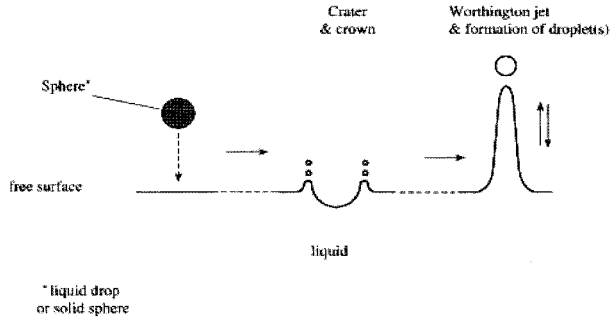

Fig. 4. Schematic representation of the splashing problem, when either a solid sphere or a liquid drop is released above the free surface of a liquid.

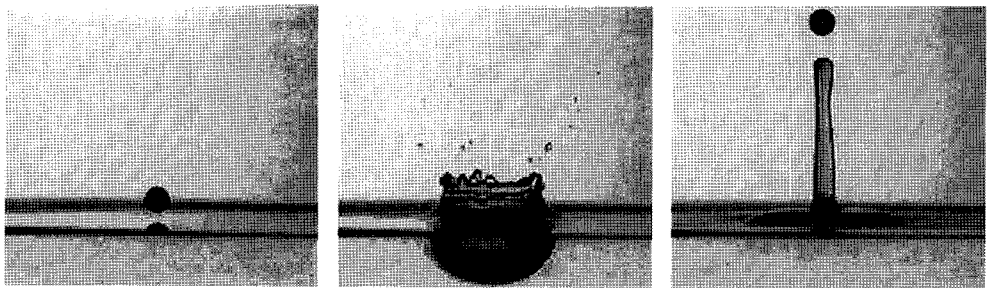

Fig. 5. The splash of a water drop (4 mm in diameter) on water (falling distance: 50 cm) (from Cheny and Walters, 1999).

absent in a given experiment. We shall be mainly interested in the vertical jet, which is called "the Worthington jet" after the scientist who first investigated the phenomenon over one hundred years ago (Worthington, 1908). This can reach extravagant heights in the case of Newtonian liquids, given the right experimental conditions.

In our previous computational studies on splashing (see, for example, Tomé *et al.*, 2007), we confined attention to the 'falling drop' situation, since this presented fewer numerical difficulties and still provided interesting insights into the general splashing phenomenon. To demonstrate that the observed flow features for this case can match those in the schematic diagram we have illustrated in Fig. 4, we show, in Fig. 5, experimental pictures for a water drop impinging on water.

One reason for the rheological interest in the Worthington jet arises from the fact that very low levels of viscoelasticity in a liquid can result in a spectacular decrease in the height of the jet (Cheny and Walters, 1996, 1999; Cheny, 1997; Nigen and Walters, 2001). Specifically, concentrations of high molecular weight polymers as low as 10Wppm, (comparable to those used in 'drag-reduction' studies), can lead to jets which are an order of magnitude lower than those observed in equivalent Newtonian liquids. This has been tentatively associated with the relatively high extensional viscosity found in very dilute polymer solutions. Indeed, the Worthington-jet experiment has even been proposed as an inexpensive monitor of extensional-viscosity levels! (Cheny and Walters, 1999).

Some experimental studies by Yang *et al.* (2000) have indicated that the situation may be more complex in the case of surfactant solutions, and the original proposal to associate low Worthington-jet heights with extensional viscosity merits further study. This provides one of the motivations for the present study.

So, the scene is set. In the two basic flow situations we have introduced, extensional viscosity has been proposed as a major influence on flow characteristics, leading to high Couette corrections in contraction flows and to reduced Worthington-jet heights in the splashing experiments.

We shall investigate these ideas in the present communication by carrying out detailed *computational* studies, all of which attempt to isolate the respective influences of extensional viscosity and other rheometrical variables on flow characteristics.

1.3. Constitutive equations and some existing numerical simulations

We now need to address the question of choosing appropriate constitutive equations for the Boger fluids we have discussed in relation to the experimental results we wish to understand and interpret.

Confining attention to incompressible Boger fluids, we can write the Cauchy stress tensor σ_{ik} in the form:

$$\sigma_{ik} = -p\delta_{ik} + T_{ik}, \tag{8}$$

where p is an arbitrary isotropic pressure, δ_{ik} the Kronecker delta, and T_{ik} is the so-called extra-stress tensor.

Constitutive equations relate the extra-stress tensor T_{ik} to a suitable kinematic variable such as the rate-of-strain tensor d_{ik}. For two specific but very different reasons, it is often convenient to introduce a so-called "stress splitting":

$$T_{ik} = T_{ik}^{(1)} + T_{ik}^{(2)}, \tag{9}$$

and to write $T_{ik}^{(1)}$ as a Newtonian contribution

$$T_{ik}^{(1)} = 2\eta_1 d_{ik}. \tag{10}$$

Computational rheologists have often found that the introduction of the Newtonian component can greatly assist in the numerical simulation of complex flows, and *experimental* rheologists, particularly those working with Boger fluids, have also found the modification to be useful. They invariably associate η_1 with the solvent viscosity.

As an example of this stress splitting, consider the well-known Oldroyd B model, with constitutive equations given by

$$T_{ik} + \lambda_1 \overset{\nabla}{T}_{ik} = 2\eta_0 [d_{ik} + \lambda_2 \overset{\nabla}{d}_{ik}], \tag{11}$$

where the triangle denotes the usual upper-convected time derivative introduced by Oldroyd (1950).

It is often convenient to write this equation in the form:

$$T_{ik}^{(1)} = 2\eta_0 \beta d_{ik} \tag{12}$$

$$T_{ik}^{(2)} + \lambda_1 \overset{\nabla}{T}_{ik}^{(2)} = 2\eta_0 (1-\beta) d_{ik},$$

where $\beta = \lambda_1/\lambda_2$.

For the popular Boger fluids, which have been used in many experimental studies (see, for example, Boger and Walters, 1993), the polymer contribution to the total viscosity is very low. This is dominated by the solvent contribution, so that β is usually in the range 0.9 to 0.95, or even higher.

The important rheometrical functions for the Oldroyd B model are given by

$$\eta = \eta_0,$$
$$N_1 = 2\eta_0(1-\beta)\lambda_1\dot{\gamma}^2, \quad N_2 = 0, \tag{13}$$
$$\eta_E = 3\beta\eta_0 + 3(1-\beta)\eta_0\left[\frac{1}{1-\lambda_1\dot{\varepsilon}-2\lambda_1^2\dot{\varepsilon}^2}\right].$$

We see that the Oldroyd B model predicts a *constant* shear viscosity η_0, a quadratic first normal stress difference N_1, a zero second normal stress difference N_2, and a potentially large extensional viscosity η_E. In fact, η_E reaches an infinite value at a finite value of the extensional strain rate, $\dot{\varepsilon}$.

As we have indicated, shear thinning is (virtually) absent in Boger fluids. Furthermore, the uniaxial extensional viscosity levels can be very high. These facts have been the main reasons for the popularity of the Oldroyd B model in Computational Rheology. The *relative* simplicity of the model is another factor of importance.

However, it needs to be stressed that all simulations for the Oldroyd B have been singularly unable to predict the large increases in the Couette correction found when Boger fluids flow through axisymmetric contraction and contraction/expansion flows (Walters *et al.*, 2008; 2009a, b).

The initial reaction of workers in the field was to question the accuracy of the numerical schemes being employed. However, this is no longer viewed as a valid criticism and simulations of the sort shown in Fig. 6 are now viewed as trustworthy. As a result, doubt has been cast on the suitability of the choice of the Oldroyd B model, and this is one of the issues we wish to address in this paper.

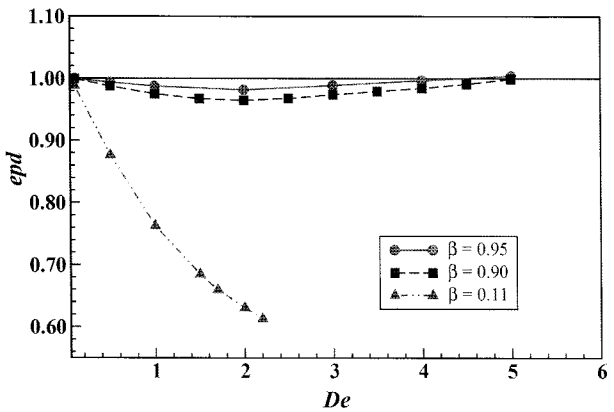

Fig. 6. Numerical pressure drop (*epd*) vs. Deborah number D_e simulations for the Oldroyd B model for three values of β (see, for example, Walters *et al.* 2009b).

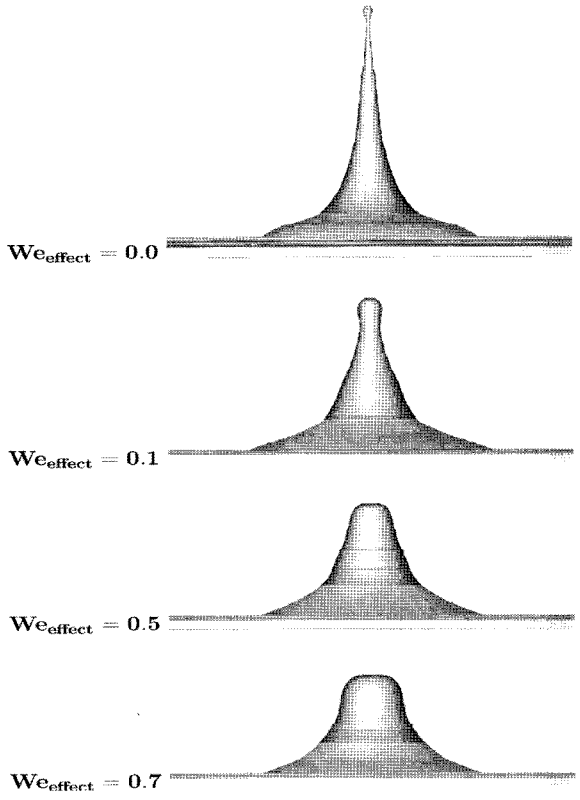

Fig. 7. Simulations of fluid flow as a function of a suitable viscoelastic flow variable at the time the Worthington jet reaches its maximum height (from Tomé *et al.* 2007).

So far as the 'splashing drop' problem is concerned, numerical results for the Oldroyd B model have recently been obtained by Tomé *et al.* (2007), and Fig. 7 is a typical figure from that publication. This shows a frontal view of the jet at its maximum height for increasing values of a suitable non-dimensional variable.

Commenting on such data, Tomé *et al.* remark: "We regard the qualitative agreement between the simulations and the experimental results of Cheny and Walters to be encouraging; indeed, the numerical technique would appear to provide a method for investigating the precise reasons for the substantial influence of viscoelasticity on the height of the Worthington jet". We shall attempt to confirm this optimism in the current paper.

2. Some constitutive-equation suggestions

We shall now draw on some of the ideas put forward by Debbaut and Crochet (1988) in an important paper that has not received the attention it deserved (Debbaut *et al.*, 1988). In these papers, use was made of two rate-of-strain invariants, which we shall conveniently refer to as $\dot{\gamma}$ and $\dot{\varepsilon}$ in what follows:

$$\dot{\gamma} = 2\sqrt{\mathbf{II}_d}, \quad \dot{\varepsilon} = 3\mathbf{III}_d/\mathbf{II}_d. \tag{14}$$

Here, $\mathbf{II}_d$ and $\mathbf{III}_d$ are the two nonzero invariants of the rate

of strain tensor d_{ik} in their usual form:

$$\mathbf{II}_d = \frac{1}{2}tr(\boldsymbol{d}^2),\ \mathbf{III}_d = det(\boldsymbol{d}). \tag{15}$$

The reason for the choice (14) instead of (15) has been fully explained by Debbaut and Crochet (1988) and Debbaut *et al.* (1988). Clearly, the invariant $\dot{\gamma}$ reduces to the usual shear rate in a steady simple shear flow and the invariant $\dot{\varepsilon}$ reduces to the usual extensional strain rate in a uniaxial extensional flow. Hence the reason for the notation.

We shall now introduce four constitutive models A-D, all of which have the structure in Eqs. (9) and (10).

Model A is simply the Newtonian fluid with $T_{ik}^{(2)}$ given by

$$T_{ik}^{(2)} = 2\eta_0(1-\beta)d_{ik}. \tag{16}$$

Model D is the Oldroyd B model we have already introduced in Eqs. (11) and (12), with rheometrical functions given in Eq. (13).

Models B and C can be seen as extensions of the models GNM1 and UCM1 in the Debbaut *et al.* (1988) papers.

B is an *inelastic* model with $T_{ik}^{(1)}$ given as in Eq. (12) and

$$T_{ik}^{(2)} = \frac{2\eta_0(1-\beta)d_{ik}}{(1-\lambda_1\dot{\varepsilon}-2(\lambda_1\dot{\varepsilon})^2)}. \tag{17}$$

The rheometrical functions for model B are

$$\begin{aligned}&\eta = \eta_0,\\ &N_1 = 0,\\ &\eta_E = 3\beta\eta_0 + 3(1-\beta)\eta_0\left[\frac{1}{1-\lambda_1\dot{\varepsilon}-2\lambda_1^2\dot{\varepsilon}^2}\right].\end{aligned} \tag{18}$$

i.e. the same η and η_E as the Oldroyd B model, but with $N_1 = 0$.

Model C has *viscoelastic* properties with $T_{ik}^{(1)}$ given as in Eq. (12) and

$$\begin{aligned}&T_{ik}^{(2)} + \lambda_1\overset{\nabla}{T}_{ik}^{(2)} = 2\eta(\dot{\gamma},\dot{\varepsilon})d_{ik},\\ &\eta(\dot{\gamma},\dot{\varepsilon}) = \eta_0(1-\beta)(1-\lambda_1\dot{\varepsilon}-2(\lambda_1\dot{\varepsilon})^2).\end{aligned} \tag{19}$$

In this case, the rheometrical functions are

$$\begin{aligned}&\eta = \eta_0,\\ &N_1 = 2\eta_0(1-\beta)\lambda_1\dot{\gamma}^2\\ &\eta_E = 3\eta_0\end{aligned} \tag{20}$$

This time it is η and N_1 that match the expressions for the Oldroyd B model, but η_E now has the Newtonian expression.

Model C can be viewed as a "Generalized White-Metzner model" (see, for example Walters *et al.*, 2009b)

The benefit of having the four A-D models available is that it allows us the luxury of the following comparisons:

1. A comparison of the simulations for models A and B provides an indication of the effect of extensional viscosity on flow characteristics, since $\eta = \eta_0$ and $N_1 = 0$ for both models.
2. A comparison of the simulations for models A and C provides an indication of the effect of "normal stresses" on flow characteristics, with a "Newtonian" extensional viscosity in both.
3. A comparison of the simulations for models B and C provides an indication of the relative strengths of normal stress and extensional viscosity effects on flow characteristics.
4. A comparison of the simulations for models C and D (*i.e.* the Oldroyd B model) highlights further the effect of a high extensional viscosity in the case of elastic liquids.
5. A comparison of the simulations for models B and D highlights further the normal stress effect, keeping in mind however that, in this comparison, model B is inelastic and model D is viscoelastic.

We feel that numerical simulations for the four constitutive models (A-D) should be able to throw considerable light on the influences of the various rheometrical functions on flow characteristics, and we discuss these issues in the next section for the two complex flows we have already highlighted. In the discussion, we recognize the limitation of using *steady* rheometrical functions in the second problem, which is of course intrinsically dynamic in character.

3. Numerical simulations for models A-D

3.1. Simulations for flow through a 4:1:4 contraction/expansion

In this section, we shall concentrate on the contraction/expansion geometry with smooth corners shown schematically in Fig. 3. We wish to obtain numerical simulations for all four models discussed in section 2 using a numerical method described in Wapperom and Webster (1998), Webster *et al.* (2004), and Belblidia *et al.* (2008). This is essentially a hybrid finite element/finite volume algorithm, which follows a three-stage time-splitting semi-implicit formulation. This scheme combines a finite element (*fe*) discretisation (Taylor-Galerkin/Pressure-Correction) for the momentum equation with a cell-vertex finite volume (*fv*) scheme for the differential constitutive laws. The combination forms a time-stepping process, with a fractional-staged formulation based upon each time-step, invoking two-step Lax-Wendroff and Crank-Nicolson time-stepping procedures. Cell-vertex *fv*-schemes applied to the stress equations are based upon an upwinding technique (fluctuation distribution) that distributes control volume residuals to provide corresponding nodal solution updates. This cell-vertex finite volume sub-element approach has proved to be an effective strategy through judicious discrete treat-

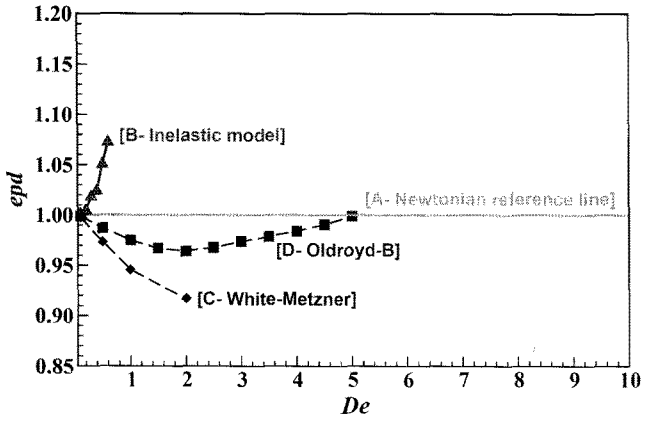

Fig. 8. Normalized pressure drop (*epd*) vs. D_e for the A-D constitutive models (cf. Walters *et al.* 2009b) ($\beta = 0.9$).

ment of flux, source and time terms of the constitutive equation.

In contrast to our work on the splashing problem in the next section, where the Reynolds number R_e is viewed as an important kinematic variable, here we shall restrict attention to "creeping flow", *i.e.* the Reynolds number is assumed to be zero.

So, we are now in a position to investigate flow in the contraction/expansion geometry using the four constitutive models (A-D) described earlier. We concentrate on the *epd* defined in Eq. (7), rather than the Couette correction, and we restrict attention to $\beta = 0.9$, although other values of β were studied in Fig. 6. The important simulations for our present purpose are all shown in Fig. 8. Note that we have included a Newtonian reference *line* on the graph, although we are aware that a Deborah number of zero is the only one of relevance in this case.

A comparison of the simulations for models A and B indicates that high extensional viscosities can give rise to significant *increases* in the *epd*.

Similarly, a comparison of the simulations for models A and C clearly indicates that the presence of normal stress differences can give rise to a *decrease* in the *epd*.

We have shown that the Oldroyd B model (Model D) has both a non-zero normal stress difference and an increasing non-Newtonian extensional viscosity and here we see a competition between the two rheometrical influences, with the extensional viscosity about to be the dominating influence at high *De*. However, we have not been able to reach the values of *De* in the simulations that would allow us to attain the expected (non-trivial) positive values of *epd*.

It is not without interest that the general shape of the curve for the Oldroyd B model is very similar to a schematic Couette correction *C* vs. Deborah number *De* diagram contained in a paper by Crochet and Walters, (1993). The associated text is revealing: "The slight drop in the Couette correction at low values of the Deborah number is difficult to measure experimentally, but most respectable numerical codes testify to its existence. The large increase in the Couette correction at high Deborah number is very easy to measure experimentally, but provides significant challenges to even the most adept numerical simulation". In many ways, this remains a valid observation!

As a general conclusion to this section, we simply remark that our numerical simulations for models A-D have confirmed earlier comments by Binding (1991) and Debbaut and Crochet (1988) that, whereas high extensional viscosity levels can give rise to large increases in the *epd*, increasing normal-stress difference levels can have the opposite effect.

3.2. Simulations for the "splashing" problem

The splashing problem introduced in section 1.2 presents computational rheologists with significant challenges. The flow is clearly unsteady in both an Eulerian and Lagrangian sense, with the shape of the free surface of the liquid changing dramatically with time. As a result, special numerical techniques have to be employed. These have been described in detail in previous papers (McKee *et al.*, 2008; Tomé *et al.* 2004; 2008) and we simply outline below their main features.

The numerical techniques employed are projection methods on a staggered grid based on the Marker and Cell technology, (McKee *et al.*, 2008). The software used is that employed for the Generalized Newtonian Model by Tomé *et al.* (2008), whilst the White-Metzner model is solved by a modification of the existing Oldroyd B code as follows:

The extensional viscosity η_E (given by (13)) is non-dimensionalized to provide

$$\bar{\eta}_E = 3\beta\bar{\eta}_0 + 3(1-\beta)\bar{\eta}_0\left[\frac{1}{1-We\bar{\dot{\varepsilon}}-2(We\bar{\dot{\varepsilon}})^2}\right], \qquad (21)$$

where $\bar{\eta}_0 = \eta_0/\eta_{\max}$, $\bar{\dot{\varepsilon}} = (L/U)\dot{\varepsilon}$ and $We = \lambda_1(U/L)$, U and L being the velocity and length scales, respectively. Since the extensional viscosity is an increasing function of $\bar{\dot{\varepsilon}}$, it can have a singularity at 0.5We and so we define

$$\eta_{\max} = 3\beta\bar{\eta}_0 + 3(1-\beta)\bar{\eta}_0\left[\frac{1}{1-We\bar{\dot{\varepsilon}}_{\max}-2(We\bar{\dot{\varepsilon}}_{\max})^2}\right], \qquad (22)$$

where $\bar{\dot{\varepsilon}}_{\max} = 0.49/We$. (Note that We is not necessarily the 'Weissenberg number' arising, for example, in studies on the Oldroyd B constitutive relationship; it is simply employed here to represent viscoelastic effects).

In the computations, it is assumed that a spherical drop of fluid is released with a specific downward velocity just above the surface of a quiescent pool of the same fluid. We have clearly needed to be selective regarding the experimental conditions to be employed in the computations, and, in the present study, we have taken:

Drop diameter (D): 10 mm; Tank dimensions: 10 cm×10 cm×4.8 cm; Fluid in the tank: 10 cm×10 cm×4 cm; Height of the drop to the pool (H): 5 mm; Velocity of the drop (U): 1.0 m/s Fluid viscosity (η_0): 0.025 Pa.s; Mesh size: $\delta x =$

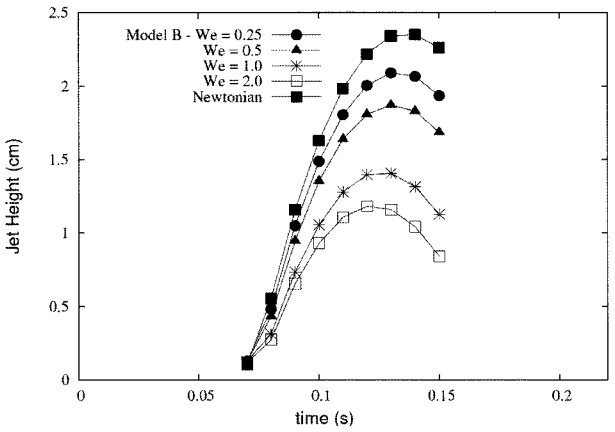

Fig. 9. Simulations of the height of the Worthington jet as a function of time for the inelastic model B ($\beta = 0.9$).

$\delta y = \delta z = 1$ mm, giving a mesh size of (100×100×80)-cells within the computational domain.

Fig. 9 contains representative simulations of the jet height versus time for the inelastic model B (*i.e.* the Generalized Newtonian Model with a high extensional viscosity). The graphs tell an obvious story, namely that, as the extensional viscosity levels increase, the maximum height of the Worthington jet decreases significantly! This is certainly consistent with the earlier suggestion of Cheny and Walters (1996; 1999) that the height of the Worthington jet can be used as a 'monitor of extensional viscosity levels'. However, before we are able to confirm the suggestion, we clearly need to address the matter in more detail. At least the data in Fig. 9 illustrate that 'extensional flow' plays an important role in the splashing experiment.

Fig. 10 is the 'splashing' equivalent of the contraction-flow data provided in Fig. 8, since it includes a meaningful comparison of the maximum heights for all four constitutive equations (A-D). We view the simulations as being revealing but also somewhat frustrating at the same time.

Clearly, all three non-Newtonian models predict lower

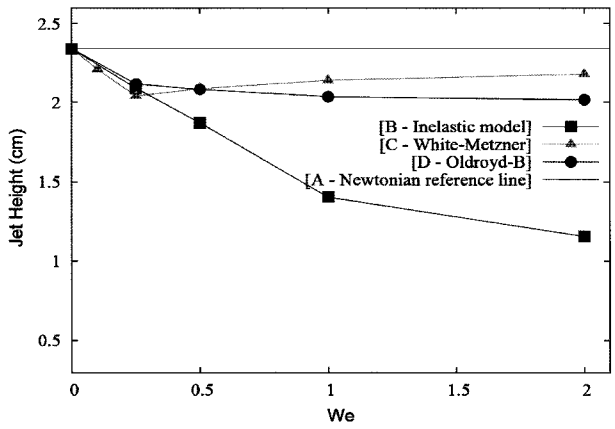

Fig. 10. Simulations of the maximum jet height of the Worthington jet as a function of We for all four constitutive models ($\beta = 0.9$).

Worthington-jet heights than that for a Newtonian liquid under the same conditions. However, the drop in height for model B, already referred to in connection with Fig. 9, is much greater than that predicted for model C, (which highlights normal stress effects). Indeed, the curve for model C goes through a minimum and the jet height is *increasing* with We at the highest values of We attainable, although we are clearly some way from predicting jet heights that are higher than the Newtonian value.

In one sense, we can anticipate that, since 'splashing' is invariably viewed as containing more 'extension' than 'shear', the curve for model B must be significantly lower than that for curve C. What is more difficult to digest and interpret is the observation that the curve for model D (the Oldroyd B model) is so near to that of model C and so far from model B. We are led to suggest (postulate) that the reason for this may lie in the fact that model B is *inelastic* (with instantaneous dependence on extensional dynamics), whilst models C and D are *viscoelastic* (introducing memory effects)! We are fully aware that the splashing experiment is manifestly 'unsteady' and viscoelasticity *per se* must play a role, independently of matters relating to 'extensional viscosity' and 'normal-stress differences'. This is something we shall wish to pursue further in the future.

We close this discussion with two comments, one positive, the other negative. First, it is clear that the curve for the Oldroyd B model lies between those for models B and C at the higher We values, and this is at least consistent with what we found in the contraction-flow simulations.

On the negative side, it is obvious that the Oldroyd B model is unable to predict the very large drops in jet height observed in splashing experiments on very dilute polymer solutions (see, for example, Cheny and Walters 1999). Again, further simulations for other more complicated constitutive models, along the lines of those considered by Walters *et al.* (2008, 2009a,b), may be in order.

4. Conclusion

In this paper, we have attempted to understand and interpret certain viscoelastic flow phenomena associated with two complex flows. By considering models A-D, we have gone some way to interpret that which is observed experimentally, but more numerical work clearly needs to be carried out before the extravagant viscoelastic effects found experimentally are interpreted theoretically.

References

Barnes, H.A., Hutton, J.F. and K. Walters, 1989, An Introduction to Rheology, *Elsevier, Amsterdam.*

Belblidia, F., Matallah, H. and M.F. Webster, 2008, Alternative subcell discretisations for viscoelastic flow: Velocity-gradient approximation, *J. Non-Newtonian Fluid Mech.* **151**, 69-88.

Binding, D.M., 1988, An approximate analysis for contraction and converging flows, *J. Non-Newtonian Fluid Mech.* **27**, 173-189.

Binding, D.M., 1991, Further considerations of axisymmetric contraction flows, *J. Non-Newtonian Fluid Mech.* **41**, 27-42.

Binding, D.M., Phillips, P.M. and T.N. Phillips, 2006, Contraction/expansion flows: The pressure drop and related issues, *J. Non-Newtonian Fluid Mech.* **137**, 31-38.

Boger, D.V., 1977/1978, A highly elastic constant-viscosity fluid, *J. Non-Newtonian Fluid Mech.* **3**, 87-91.

Boger, D.V. and Walters, K., 1993, Rheological Phenomena in Focus, *Elsevier Science Publishers.*

Castelo, A., Tomé, M.F., Cesar, C.N.L, McKee, S., and J.A. Cuminato, 2000, Freeflow: An integrated simulation system for three-dimensional free surface flows, *Computing and Visualization in Science,* **2**, 199-210.

Cheny, J-M. and. K. Walters, 1996, Extravagant viscoelastic effects in the Worthington jet experiment, *J. Non-Newtonian Fluid Mech.* **67**, 125-135.

Cheny, J-M., Ph.D. thesis, University of Wales, 1997.

Cheny, J-M. and K. Walters, 1999, Rheological influences on the splashing experiment, *J. Non-Newtonian Fluid Mech.* **86**, 185-210.

Cogswell, F.N., 1972, Measuring the extensional rheology of polymer melts, *Tran. Soc. Rheo.* **16**, 383-403.

Crochet, M.J. and K. Walters, 1993, Computational Rheology: a new science, Endeavour, **17**(2), 64-77.

Debbaut, B. and M.J. Crochet, 1988, Extensional effects in complex flows, *J. Non-Newtonian Fluid Mech.* **30**, 169-184.

Debbaut, B., Crochet, M.J., Barnes, H.A. and K. Walters, 1988, Extensional effects in inelastic liquids, Proc. *Xth Inter. Congress on Rheology, Sydney,* 291-293.

Jackson, K.P., Walters, K. and R.W. Williams, 1984, A rheometrical study of Boger fluids, *J. Non-Newtonian Fluid Mech.* **14**, 173-188.

McKee, S., Tomé, M.F., Ferreira, V.G., Cuminato, J.A., Castelo, A., and F.S. de Sousa, 2008, The MAC method, *Computers and Fluids* **37**, 907-930.

Nigen, S. and K. Walters, 2001, On the two-dimensional splashing experiment for Newtonian and slightly elastic liquids, *J. Non-Newtonian Fluid Mech.* **97**, 233-250.

Nigen, S. and K. Walters, 2002, Viscoelastic contraction flows: comparison of axisymmetric and planar configurations, *J. Non-Newtonian Fluid Mech.* **102**, 343-359.

Oldroyd, J.G., 1950, On the formulation of rheological equations of state, *Proc. Roy. Soc.* **A200**, 523-541.

Rothstein, J.P. and G.H. McKinley, 2001, The axisymmetric contraction-expansion: the role of extensional rheology on vortex growth dynamics and the enhanced pressure drop, *J. Non-Newtonian Fluid Mech.* **98**, 33-63.

Tanner, R.I. and K. Walters, *1998,* Rheology, an Historical Perspective, *Elsevier Science & Technology, Netherlands.*

Tomé, M.F., Castelo, A., Ferreira, V.G. and S. McKee, 2008, A finite difference technique for solving the Oldroyd B model for 3D unsteady free surface flows, *J. Non-Newtonian Fluid Mech.* **154**, 179-206.

Tomé, M.F., Grossi, L., Castelo, A., Cuminato, J.A., Mangiavacci, N., Ferreira, V.G., de Sousa, F.S., and S. McKee, 2004, A numerical method for solving three-dimensional generalized Newtonian free surface flows, *J. Non-Newtonian Fluid Mech.* **123**, 83-103.

Tomé, M.F., Grossi, L., Castelo, A., Cuminato, J.A., McKee, S., and K. Walters, 2007, Die-swell, splashing drop and a numerical technique for solving the Oldroyd B model for axisymmetric free surface flows, *J. Non-Newtonian Fluid Mech.* **141**, 148-166.

Walters, K., 1980, Introduction, in 'Rheometry: Industrial Applications'. Ed. K. Walters, Research Studies Press, p13.

Walters, K., Webster, M.F. and H.R. Tamaddon-Jahromi, 2008, Experimental and Computational aspects of some contraction flows of highly elastic liquids and their impact on the relevance of the Couette correction in extensional Rheology, Proc. 2nd Southern African Conference on Rheology (SASOR 2), 1-6.

Walters, K., Webster, M.F. and H.R. Tamaddon-Jahromi, 2009a, The numerical simulation of some contraction flows of highly elastic liquids and their impact on the relevance of the Couette correction in extensional rheology, *Chem Eng Sci.* **64**, 4632-4639.

Walters, K., Webster, M.F. and H.R. Tamaddon-Jahromi, 2009b, The White-Metzner model : Then and Now, Proceedings of the 25th Annual Meeting of the PPS meeting, Goa, India, IL 02, 1-14.

Wapperom, P. and M.F. Webster, 1998, A second-order hybrid finite-element/volume method for viscoelastic flows, *J. Non-Newtonian Fluid Mech.* **79**, 405-431.

Webster, M.F., Tamaddon-Jahromi, H.R. and M. Aboubacar, 2004,. Transient viscoelastic flows in planar contractions, *J. Non-Newtonian Fluid Mech.* **118**, 83-101.

Worthington, M.A., 1908, A Study of Splashes, Longmans, Green and Co., London.

Yang, F., Qi, Y., Morales, W., Hart, D.J. and J.L. Zakin, 2000, Effect of surfactant additive composition on Worthington jet splashing, Proceedings of the 13th International Congress on Rheology, Vol. **2**, Cambridge, UK, Paper 2-274.